Inhibition and pH Dependence of Phosphite Dehydrogenase†

Heather A. Relyea, Jennifer M. Vrtis, Ryan Woodyer, Stacey A. Rimkus, and Wilfred A. van der Donk*

Department of Chemistry, University of Illinois, 600 South Mathews Avenue, Urbana, Illinois 61801

Received November 6, 2004; Revised Manuscript Received February 7, 2005

ABSTRACT: Phosphite dehydrogenase (PTDH) catalyzes the NAD-dependent oxidation of phosphite to phosphate, a reaction that is 15 kcal/mol exergonic. The enzyme belongs to the family of D-hydroxy acid dehydrogenases. Five other family members that were analyzed do not catalyze the oxidation of phosphite, ruling out the possibility that this is a ubiquitous activity of these proteins. PTDH does not accept any alternative substrates such as thiophosphite, hydrated aldehydes, and methylphosphinate, and potential small nucleophiles such as hydroxylamine, fluoride, methanol, and trifluoromethanol do not compete with water in the displacement of the hydride from phosphite. The pH dependence of $k_{cat}/K_{m,phosphite}$ is bell-shaped with a pK_a of 6.8 for the acidic limb and a pK_a of 7.8 for the basic limb. The pK_a of 6.8 is assigned to the second deprotonation of phosphite. However, whether the dianionic form of phosphite is the true substrate is not clear since a reverse protonation mechanism is also consistent with the available data. Unlike $k_{cat}/K_{m,phosphite}$, k_{cat} and $k_{cat}/K_{m,NAD}$ are pH-independent. Sulfite is a strong inhibitor of PTDH that is competitive with respect to phosphite and uncompetitive with respect to NAD^+. Incubation of the enzyme with NAD^+ and low concentrations of sulfite results in a covalent adduct between NAD^+ and sulfite in the active site of the enzyme that binds very tightly. Fluorescent titration studies provided the apparent dissociation constants for NAD^+, NADH, sulfite, and the sulfite−NAD^+ adduct. Substrate isotope effect studies with deuterium-labeled phosphite resulted in small normal isotope effects (1.4−2.1) on both k_{cat} and $k_{cat}/K_{m,phosphite}$ at pH 7.25 and 8.0. Solvent isotope effects (SIEs) on k_{cat} are similar in size; however, the SIE of $k_{cat}/K_{m,phosphite}$ at pH 7.25 is significantly larger (4.4), whereas at pH 8.0, it is the inverse (0.6). The pH−rate profile of $k_{cat}/K_{m,phosphite}$, which predicts that the observed SIEs will have a significant thermodynamic origin, can account for these effects.

Phosphite dehydrogenase (PTDH)[1] from *Pseudomonas stutzeri* WW88 is a unique NAD^+-dependent enzyme that oxidizes inorganic phosphite (hydrogen phosphonate) to phosphate (eq 1).

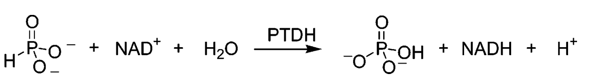

(1)

The enzyme allows this organism to grow on phosphite as its sole phosphorus source (*1*−*3*). The oxidation of phosphite resembles a phosphoryl transfer reaction in which water or hydroxide is the phosphoryl acceptor. However, sequence alignments reveal that the sequence of PTDH is 26−35% identical with the sequence of the D-hydroxy acid dehydrogenase family of enzymes (*2*). Importantly, the three catalytic residues that are conserved throughout this family are also found in PTDH (Figure 1), providing clues about how the enzyme promotes its unusual transformation. The roles of these residues, Arg237, His292, and Glu266 (PTDH numbering), have been investigated in several D-hydroxy acid dehydrogenases, leading to a model in which arginine binds the carboxylate moiety of the substrate, histidine acts as a catalytic acid in the physiologically important direction of substrate reduction, and glutamate plays a role in modulation of the pK_a of the active site histidine to keep it protonated for substrate binding (Figure 2A) (*4*−*8*).

These roles can be directly projected onto the PTDH reaction with the important difference that its physiological role is substrate oxidation ($K_{eq} \sim 10^{11}$ in favor of phosphate) (Figure 2B). Site-directed mutagenesis studies (*9*) provide support for a role for arginine in binding phosphite and for His292 as the active site base (or nucleophile; see below). In addition a second basic residue, Lys76, identified in a homology model for the structure of PTDH (*10*), is involved in phosphite binding (*9*). The role of Glu266 is less well defined, but it does not appear to serve to keep His292 in its protonated state as found in most other dehydrogenases (DHs) (*9*). In addition to the mechanism in Figure 2B, PTDH may utilize a covalent mechanism in which an enzyme nucleophile initially displaces the hydride leaving group followed by hydrolysis of the phosphoenzyme intermediate

† Support for this research was provided by the National Institutes of Health (Grant GM 63003) and the Camille Dreyfus Teacher-Scholar Awards Program.

* To whom correspondence should be addressed. Phone: (217) 244-5360. Fax: (217) 244-8024. E-mail: vddonk@uiuc.edu.

[1] Abbreviations: DH, dehydrogenase; DGDH, D-glycerate dehydrogenase; $^{D}k_{cat}$, substrate deuterium kinetic isotope effect on k_{cat}; $^{D}(k_{cat}/K_{m,Pt})$, substrate deuterium kinetic isotope effect on $k_{cat}/K_{m,Pt}$ for phosphite; DLDH, D-lactate dehydrogenase; DPGDH, D-3-phosphoglycerate dehydrogenase; D-Pt, deuterium-labeled phosphite; FPLC, fast protein liquid chromatography; FDH, formate dehydrogenase; HPLC, high-performance liquid chromatography; IMAC, immobilized metal affinity chromatography; IPTG, isopropyl β-D-thiogalactopyranoside; KIE, kinetic isotope effect; NAD^+ and NADH, nicotinamide adenine dinucleotide; H-Pt, phosphite; PTDH, phosphite dehydrogenase; SIE, solvent isotope effect; wt, wild-type.

10.1021/bi047640p CCC: $30.25
Published on Web 04/06/2005

```
PTDH  GCALKGFDNFDVDACTARGVWLTFVPDLLTVPTAELAIGLAVGLGRHLRAADAFVRSGEF 131
DGDH  STYSIGFDHIDLDACKARGIKVGNAPHGVTVATAEIAMLLLLGSARRAGEGEKMIRTRSW 133
PGDH  GCFCIGTNQVDLDAAAKRGIPVFNAPFSNTRSVAELVIGELLLLLRGVPEANAKAHRGVW 139
DLDH  SLRNVGVDNIDMDKAKELGFQITNVPVYSPNAIAEHAAIQAARVLRQDKRMDEKMAKRDL 134
FDH   LTAGIGSDHVDLQSAIDRNVTVAEVTYCNSISVAEHVVMMILSLVRNYLPSHEWARKGGW 178
           G    D                      AE          R

PTDH  QGWQP-QFYGTGLDNATVGILGMGAIGLAMADRLQGWGATLQYHEAKALDTQTEQRLGLR 190
DGDH  PGWEPLELVGEKLDNKTLGIYGFGSIGQALAKRAQGFDMDIDYFDTHRASSSDEASYQAT 193
PGDH  NKLAAGSFEAR---GKKLGIIGYGHIGTQLGILAESLGMYVYFYDIENKLPLGNATQVQH 196
DLDH  R-WAP--TIGREVRDQVVGVVGTGHIGQVFMRIMEGFGAKVIAYDIFKNPELEKKGYYVD 191
FDH   N-IADCVSHAYDLEAMHVGTVAAGRIGLAVLRRLAPFDVHLHYTDRHRLPESVEKELNLT 237
                        G  g G  G                 d

PTDH  -QVACSELFASSDFILLALPLNADTQHLVNAELLALVRPGALLVNPCRGSVVDEAAVLAA 249
DGDH  FHDSLDSLLSVSQFFSLNAPSTPETRYFFNKATIKSLPQGAIVVNTARGDLVDNELVVAA 253
PGDH  ----LSDLLNMSDVVSLHVPENPSTKNMMGAKEISLMKPGSLLINASRGTVVDIPALCDA 252
DLDH  ---SLDDLYKQADVISLHVPDVPANVHMINDKSIAEMKDGVVIVNCSRGRLVDTDAVIRG 248
FDH   WHATREDMYPVCDVVTLNCPLHPETEHMINDETLKLFKRGAYIVNTARGKLCDRDAVARA 297
                      L  P                   G    N  RG   D      .

PTDH  LERGQLGGYAADVFEMED------WARADRPRLIDPALLAHPN-TLFTPHIGSAVRAVRL 302
DGDH  LEAGRLAYAGFDVFAGE--------------PNINEGYYDLPN-TFLFPHIGSAATQARE 298
PGDH  LASKHLAGAAIDVFPTEP---------ATNSDPFTSPLCEFDN-VLLTPHIGGSTQEAQE 302
DLDH  LDSGKIFGFVMDTYEDEVGVFNKDWEGKEFPDKRLADLIDRPN-VLVTPHTAFYTTHAVR 307
FDH   LESGRLAGYAGDVWFPQP-----------APKDHPWRTMPYNG---MTPHISGTTLTAQA 343
      L          D    e                               PH
```

FIGURE 1: Partial sequence alignment of PTDH with members of the D-hydroxy acid dehydrogenase family. In yellow are three residues, Arg237, Glu266, and His292 (PTDH numbering), that have important catalytic functions in the hydroxy acid dehydrogenases (*5*, *54*, *55*). A Lys residue (red) that is located in the active site of a homology model of PTDH (*9*, *10*) is not conserved in other members of the family with known D-hydroxy acid dehydrogenase activity. Abbreviations (% identity with PTDH, GenBank accession number): DGDH, D-glycerate DH (*H. methylovorum*, 27%, P36234) (*56*); DPGDH, D-3-phosphoglycerate DH (*E. coli*, 24%, P08328) (*57*); DLDH, D-lactate DH (*Lactobacillus helveticus*, 26%, P30901) (*58*); and FDH, formate DH (*Pseudomonas* sp. 101, 25%, P33160) (*59*).

(Figure 2C). Glu266 has been ruled out as the enzyme nucleophile since mutation to Gln resulted in an active mutant enzyme (*9*). On the other hand, the available experimental evidence does not rule out such a role for His292.

It is highly unusual for a dehydrogenase to catalyze a nucleophilic displacement reaction. Hydride would normally be an exceptionally poor leaving group for such a transformation, but a strong driving force is provided by the very favorable thermodynamics of oxidizing phosphite to phosphate ($E^{\circ\prime} = -0.648$ V) while reducing NAD^+ to NADH ($E^{\circ\prime} = -0.320$ V), a process that is overall ~15 kcal/mol exergonic. One question raised by the very favorable energetics as well as the lack of previous reports on the presence of phosphite in biological systems is whether phosphite is the actual substrate for the enzyme. A related question is whether other DHs can catalyze the same reaction. In this contribution, we present the results of studies that start to provide experimental insights into the catalytic process, including the enzyme's substrate specificity, the pH dependence of its steady-state kinetic parameters, substrate and solvent kinetic isotope effects, and the affinity of the enzyme for its substrates.

EXPERIMENTAL PROCEDURES

Materials

Phosphorous acid was purchased from Aldrich. D-Lactate dehydrogenase from *Lactobacillus leichmannii*, 3-phosphoglycerate dehydrogenase from chicken liver, formate dehydrogenase from *Candida boidinii*, and NAD^+ were purchased from Sigma. The gene encoding glycerate dehydrogenase from *Hyphomicrobium methylovorum* was isolated, cloned into pRW2 (*10*), and expressed recombinantly in *Escherichia coli*. All chemicals for the synthesis of thiophosphite and methylphosphinic acid were purchased from either Aldrich or Fisher. Expression and purification of His-tagged PTDH have been reported previously (*10*).

Methods

Concentrations of NAD^+ solutions were determined by the absorbance at 260 nm (ϵ = 18 mM^{-1} cm^{-1}). To determine the concentrations of phosphite (H-Pt) or deuterium-labeled phosphite (D-Pt) stock solutions, they were diluted to approximately 160 μM. The solution was then mixed in a known proportion with a solution of 0.5−1 mM NAD^+, and PTDH was added. The reaction was allowed to proceed to completion. The maximum absorbance reached at 340 nm was recorded, representing the concentration of NADH formed (ϵ = 6.2 mM^{-1} cm^{-1}), which is equivalent to the amount of phosphite consumed.

General Activity Assays for PTDH. All activity assays were performed on a Cary 100 Bio UV−Vis instrument as described previously (*10*). A total reaction volume of 0.5 mL was used in a 1.0 mL quartz cuvette (path length of 1 or 10 cm). All reactions were carried out at 25 °C by storing samples in a 25 °C water bath and using a jacketed cuvette

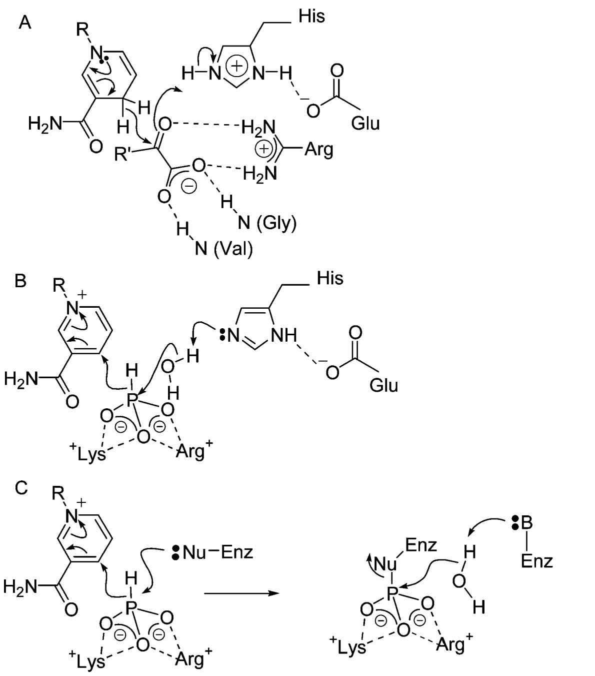

FIGURE 2: (A) Schematic representation of the roles of the conserved active site residues in D-hydroxy acid dehydrogenases. (B) Extrapolation of the mechanism in panel A to phosphite dehydrogenase. In this model, the water nucleophile occupies the same position as the hydroxyl group of D-hydroxy acids. (C) Involvement of an active site residue in covalent catalysis in PTDH. The drawings are not intended to distinguish between associative, dissociative, or concerted mechanisms of nucleophilic substitution and are not intended to indicate the stereochemical outcome of the reaction. For a discussion of the currently unknown details of the reaction, see ref *51*.

holder. Reactions were initiated with the addition of PTDH, and the absorbance at 340 nm was monitored for 60 s.

Screen for Activity of D-Hydroxy Acid Dehydrogenases with Phosphite. Solutions of 100 mM phosphite and 4 mM NAD^+ were treated with 5−70 μg of enzyme at room temperature in Tris at pH 9.0 (DPGDH and DGDH) or MOPS at pH 7.5 (DLDH and FDH). The pH of these experiments was chosen such that the enzyme under investigation has maximal activity for oxidation of 2-hydroxy acids. Absorbance at 340 nm was recorded periodically over a 6 h period and compared with that of a nonenzymatic control. The rates of the control and enzymatic reactions were essentially identical (4×10^{-4} mM^{-1} s^{-1}). To ensure that the enzymes displayed the expected activities with their native substrates, the corresponding kinetic parameters were determined. For DPGDH, $k_{cat} = 0.3$ s^{-1}, $K_{m,D-phosphoglycerate} = 460$ μM, and $K_{m,NAD} = 24$ μM. For DGDH (partially purified), $k_{cat} = 2.2$ s^{-1}, $K_{m,D-glycerate} = 530$ μM, and $K_{m,NAD} = 110$ μM. For FDH, $k_{cat} = 1.8$ s^{-1}, $K_{m,formate} = 2.8$ mM, and $K_{m,NAD} = 128$ μM. For DLDH, $k_{cat}/K_{m,D-lactate} = 2.0 \times 10^3$ M^{-1} s^{-1} [this enzyme could not be saturated in D-lactate; a $K_{m,lactate}$ of up to 130 mM has been observed for the enzyme from another *Lactobacillus* species (*11*)]. The measured values agreed well with literature values (*12, 13*).

Screen for Activity of PtxD with Alternative Substrates. Solutions of 10 mM paraformaldehyde, glyoxal, glycolic acid, or glyoxylic acid were made in 10 mL of 30 mM phosphate buffer at pH 7.25. NAD^+ was added to a final concentration of 10 mM. PTDH (120 μg, final concentration of 0.3 μM) was added, and the mixture was incubated at room temperature for several hours. The protein was then removed by passing the reaction mixture through a Centricon YM30 membrane. The flow-through was lyophilized, redissolved in D_2O, and analyzed by ^{1}H NMR spectroscopy because any NADH produced via the oxidation of these compounds might not be able to be detected spectroscopically as it could be used by the protein to also reduce the substrate (disproportionation). However, neither oxidized nor reduced products were observed by NMR spectroscopy, indicating these compounds are not substrates for PTDH.

pH Profiles for PTDH. Solutions of 100 mM Tris, 50 mM MES, and 50 mM AcOH (a universal buffer of constant ionic strength) (*14*) were adjusted to the following pH values at 25 °C using 5 M NaOH or 5 M HCl: 5.5, 5.8, 6.0, 6.3, 6.5, 6.7, 7.0, 7.3, 7.7, 8.0, 8.2, 8.4, 8.7, 9.0, and 9.5. Stock solutions of NAD^+ and phosphite were made in each of the buffer solutions. The NAD^+ concentration was held at 2 mM over the entire range (saturating conditions), while phosphite concentrations were varied to determine $k_{cat}/K_{m,phosphite}$. The pH dependence of $k_{cat}/K_{m,NAD^+}$ was determined by holding the phosphite concentration at $10K_{m,Pt}$ and varying the NAD^+ concentration from 0.05 to 1.0 mM. Reactions were initiated by adding 1.5−3.5 μg of PTDH. A similar strategy was followed to determine the pH dependence of the K_i of sulfite in the presence of 100 μM NAD^+ and varying concentrations of phosphite.

Data Analysis for pH Profiles. Raw rate data at each pH were analyzed using the Michaelis−Menten equation to obtain values of k_{cat}, K_m, and k_{cat}/K_m. The resulting rate data were converted to log form and plotted against pH. These data were fit using nonlinear regression analysis to eq 2 (*15*). The resulting values for pK_{a1} and pK_{a2} are relatively close and therefore may not represent the true microscopic pK_a values (*16*). For the inhibition data, the same equation was used substituting $-\log K_i$ for $\log(V/K)$. The constants $(V/K)_0$ and $(K_i)_0$ represent the plateau value at optimum pH.

$$\log(V/K) = \log\left[\frac{(V/K)_0}{1 + \frac{[H^+]}{K_a} + \frac{K_{a'}}{[H^+]}}\right] \qquad (2)$$

Spectroscopic Analysis of the Reaction of Sulfite, NAD^+, and PTDH. In two independent experiments, a solution containing 60 μM PTDH and 1 mM NAD^+ was treated with aliquots of an 8 mM sulfite solution. The reaction resulted in an increase in the absorbance at 310 nm (λ_{max}), which was not observed in the absence of PTDH. Using an extinction coefficient of 4.8 mM^{-1} cm^{-1} at 320 nm for a chemical adduct between sulfite and NAD^+ (*17*), the species was formed in 50 μM when 1 equiv of sulfite had been added with respect to the enzyme.

Preparation of Deuterium-Labeled Phosphite. Deuterium-labeled phosphite was prepared by mixing phosphorous acid with deuterium oxide at 25 °C for ∼6−12 h, evaporating the D_2O on a rotary evaporator, and again dissolving the phosphorous acid in deuterium oxide. This was repeated several times until only deuterium-labeled phosphite was present in solution as determined by ^{31}P NMR spectroscopy (500 MHz Varian, H_3PO_4 as an external reference δ 0 ppm): D_3PO_3 δ 5.48 (t, J_{P-D} = 103 Hz), H_3PO_3 δ 5.75 (d, J_{P-H} = 674 Hz).

Substrate and Solvent Kinetic Isotope Effects. Stock solutions of NAD^+ and deuterium-labeled or unlabeled phosphite in 50 mM MOPS (pH 7.25) [or 50 mM Tris (pH 8.0)] were aliquoted into two tubes with equal volumes, lyophilized, and resuspended in either H_2O or D_2O. The pH (pD) was adjusted to 7.25 or 8.0 (pD = $pH_{meter\ reading}$ + 0.4) (*18*). For solutions in D_2O, the pD was adjusted with DCl or NaOD. Solutions in Tris buffer were placed in a water bath at 25 °C, immediately prior to adjustment of the pH (pD) because the pH of Tris buffer fluctuates with temperature (*19*). When the pH (pD) was measured for the Tris solutions, a thermocouple was in the solution to verify that the temperature was 25 °C. The stock solutions at pH (pD) 7.25 were aliquoted and mixed to provide 36 solutions with six fixed concentrations of NAD^+ and six varied concentrations of phosphite (labeled or unlabeled) in H_2O or D_2O. Similarly, the stock solutions at pH (pD) 8.0 were aliquoted and mixed to provide 25 solutions with five varied concentrations of NAD^+ and five varied concentrations of phosphite (labeled or unlabeled) in H_2O or D_2O. These solutions were used for activity assays, and the data were analyzed with a modified version of Cleland's program (*20*, *21*). The kinetic parameters V_{max} and K_m for both phosphite and NAD^+ were obtained by fitting the data to a sequential ordered mechanism with NAD^+ binding first. In principle, differences in viscosity (η_{D_2O}/η_{H_2O} = 1.2 at 25 °C) (*22*) can affect the SIE, and hence, the influence of viscosity was investigated using glycerol as a microviscogen. The relative viscosities ($\eta_{rel} = \eta/\eta^0$) of D_2O and several glycerol concentrations in H_2O were measured with a viscometer (TA Instruments Rheometer AR 1000 N) at 25 °C in 50 mM MOPS buffer (pH 7.25) with the same solution without the viscogen as the reference. A solution of 6% glycerol provided the same relative viscosity ($\eta_{6\%\ glycerol}/\eta_{H_2O}$ = 1.2) at 25 °C as D_2O.

Determination of Binding Constants by Fluorescence Quenching. Fluorescence titration experiments were performed with 200 μL of His_6-tagged PTDH dimer in 50 mM MOPS buffer adjusted to a pH of 7.25. The intrinsic tryptophan fluorescence was measured with an excitation wavelength of 295 nm (2.5 nm slit width) while monitoring the emission spectrum from 310 to 380 nm (2.5 nm slit width). All fluorescence measurements were taken on a Fluoromax-2 instrument (ISA-Jobin Yvon SPEX, Edison, NJ) using a 0.2 cm × 1 cm quartz cuvette (1 cm side facing the emission filter). For NAD^+ and NADH titrations, a protein concentration of 2.5 μM (dimer) was used for enhanced signal, while for the combination of sulfite and NAD^+ titrations, a concentration of 0.5 μM was used to facilitate measurement of the lower apparent K_D values. An intermediate protein concentration of 1.25 μM (dimer) was used in the case of sulfite titration in the absence of cofactor. Varying amounts of cofactor or sulfite prepared in the same buffer were added to the protein samples. The total sample volume was never diluted more than 7.5% over the entire titration, and both intensities and concentrations were corrected for the actual dilution. In the case of ordered binding experiments, either 0.2 mM NAD^+ or 0.2 mM sulfite was added prior to the titration with the other substrate. All titrations were carried out at room temperature (25 °C) and in triplicate. The fluorescence of the buffer solution was used as a baseline blank. In the case of NADH titration, the large absorbance at 340 nm coincides with the λ_{max} emission of the protein, and thus, the spectra were further corrected for the inner filter effect (*23*). Binding constants were determined by plotting the corrected change in λ_{max} emission at 340 nm against the concentration of the titrant. The data were fit to a single-binding site equation using Origin 5.0 Professional nonlinear regression analysis (Table 1). Using the ΔF_{max} value obtained from this analysis, Scatchard analysis was also performed assuming that the maximal change in fluorescence corresponds with all binding sites being occupied. The Scatchard analysis takes into consideration the concentration of acceptor as well as the ligand and provided numbers similar to those from the nonlinear regression analysis.

Table 1: Apparent Dissociation Constants from Fluorescence Quenching Experiments

ligand	K_D (μM)	ligand	K_D (μM)
NAD^+	11.3 ± 0.8	sulfite	330 ± 50
NADH	30 ± 5	sulfite (NAD^+)[b]	0.76 ± 0.04
NAD^+ (sulfite)[a]	0.61 ± 0.03		

[a] Apparent binding constant of NAD^+ at a sulfite concentration of 0.2 mM. [b] Apparent binding constant of sulfite at saturating NAD^+ concentrations.

RESULTS

Is Phosphite Oxidation a Fortuitous Activity of PTDH? Given the strong thermodynamic driving force for oxidation of phosphite to phosphate while reducing NAD^+ to NADH, the potential of other members of the D-hydroxy acid DH family to catalyze this transformation was investigated. D-Lactate dehydrogenases from *L. leichmannii* and *Lactobacillus bulgaricus*, 3-phosphoglycerate dehydrogenase from chicken liver, glycerate dehydrogenase from *Hyphomicrobium methylovorum*, and formate dehydrogenase from *Candida boidinii* did not display any detectable activity as judged by the absorbance at 340 nm (λ_{max} of NADH) in the presence of 100 mM phosphite and 4 mM NAD^+ after incubation for 6 h (5−70 μg of protein). The activity of these enzymes with their native substrates was also measured as a control and corresponded well with the published values (Experimental Procedures). These results show that phosphite is not a promiscuous substrate for this class of enzymes. The specificity for phosphite is not imparted just by the presence of Lys76, which has been shown to be involved in phosphite binding (*9*) and is absent in the DHs tested above. Mutation of Ile/Val76 to Lys (PTDH numbering) in glycerate DH from *H. methylovorum* and D-lactate DH from *L. bulgaricus* did not result in mutants with PTDH activity.

Substrate Specificity. Although these results suggest that phosphite oxidation activity is unique to PTDH, it does not necessarily rule out another substrate in physiological settings. To expand the series of alternative substrates that were tested in a previous study (*2*), a number of additional potential substrates was evaluated. Alkyl hydrogen phosphinates, $RHP(=O)O^-$, are found naturally in the biosynthetic pathways of several natural products (*24*), and they might constitute substrates for PTDH in a salvage pathway. These compounds formally contain phosphorus in the +1 oxidation state, and NAD^+-dependent oxidation to the corresponding alkyl phosphonate (+3 valence on P) would be analogous to the oxidation of phosphite to phosphate (+3 to +5 valence) in that it involves replacement of a hydride with a hydroxyl group. As the sterically least demanding member of this class of compounds, methyl phosphinate was prepared according to literature procedures (*25*). When the compound was incubated with PTDH and NAD^+, no reaction was observed. Thiophosphite was also prepared (*26*) as a potential mechanistic probe for evaluation of any element effects. Unlike phosphate monoesters, thiophosphate monoesters have been shown to react in solution via a thiometaphosphate intermediate (*27*−*31*). However, somewhat surprisingly, PTDH did not catalyze the NAD^+-dependent oxidation of thiophosphite. Another potential substrate that did not display any activity was fluorophosphate, which was envisioned as a potential active site labeling reagent, especially if PTDH uses covalent catalysis. In addition to not exhibiting any catalytic activity, none of these compounds substantially inhibited PTDH.

Another set of potential substrates that were evaluated involved compounds containing aldehyde functionalities. These are (partially) hydrated in aqueous solution and might resemble the tetrahedral phosphite molecule. Furthermore, there is precedent for the oxidation of hydrated aldehydes by L-lactate dehydrogenase, which oxidizes the hydrated form of glyoxylate to oxalate (*32*−*35*). However, in this study, glyoxylate, glyoxal, glycolate, and formaldehyde were not oxidized or reduced by PTDH. We therefore conclude that the enzyme is highly specific for phosphite. Attempts to make the enzyme accept nucleophiles other than water by adding high concentrations of methanol, trifluoromethanol, hydroxylamine, or fluoride ion resulted in production of only the native phosphate product rather than phosphate esters/amides or fluorophosphate.

pH Dependence of Steady-State Kinetic Parameters. PTDH activity was assayed at several concentrations of phosphite in the presence of saturated concentrations of NAD^+ over a pH range from 5.5 to 9.5. As depicted in Figure 3A, k_{cat} is essentially independent of pH. This independence is also observed for $k_{cat}/K_{m,NAD^+}$ (see the Supporting Information). However, $k_{cat}/K_{m,phosphite}$ exhibits a clear dependence on pH (Figure 3B). From the data, pK_a values for the enzyme−NAD^+ complex of 6.8 ± 0.1 and 7.8 ± 0.2 were determined. The experimental values for $k_{cat}/K_{m,phosphite}$ indicate a very small pH range (<1 unit) centered around pH 7.25 in which the enzyme is most active. Above and below this range, dehydrogenase activity drops off steeply. The slope of each arm of the profile is unity, indicating that one proton transfer transition is responsible for the observed activity changes in these pH ranges.

pH Profile of the K_i of Sulfite. To positively assign the acidic limb of the pH−rate profile of $k_{cat}/K_{m,phosphite}$ to the second deprotonation of phosphorous acid (pK_a = 6.8), a pH profile of K_i for sulfite was obtained in the presence of NAD^+ at concentrations near its K_m at each pH. Sulfite is a strong inhibitor of PTDH that is competitive with respect to phosphite (*2*). By determining the rate of reaction at various concentrations of phosphite and sulfite, one can extrapolate the binding constant (K_i) for sulfite in the absence of substrate. This value represents binding of the inhibitor to the enzyme (*15*, *16*), and if sulfite binds in a fashion similar to that of phosphite, as suggested by its competitive inhibition

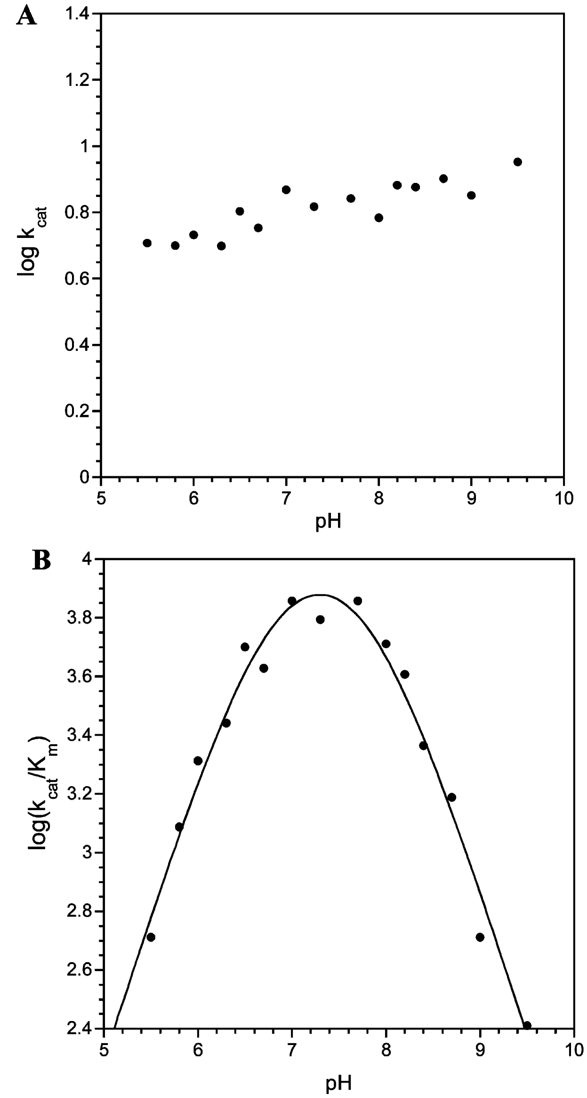

FIGURE 3: pH dependence of (A) k_{cat} and (B) $k_{cat}/K_{m,phosphite}$. The solid line was drawn by fitting the data to eq 2 (Experimental Procedures).

profile, its pH−inhibition profile should reflect the second deprotonation of sulfurous acid. The pH−pK_i profile displays a shape similar to that of $k_{cat}/K_{m,phosphite}$ (Figure 4). The data were fitted to eq 2 to extract quantitative values for the proton transfer transitions. One transition occurred at a pK_a of 6.4 ± 0.1, whereas the basic limb corresponded to a pK_a of 8.4 ± 0.2.

Formation of a Covalent Adduct of NAD^+ and Sulfite. Spectroscopic analysis of the titration of sulfite into a solution containing a high concentration of PTDH (60 μM) and a saturating concentration of NAD^+ (1 mM) revealed an increase in the absorbance around 310 nm. Formation of a NAD^+−sulfite adduct has been observed previously, and an extinction coefficient has been reported for the adduct (*17*). Using this value, the adduct was generated in ~85% yield when equal amounts of PTDH and sulfite were present. In a control experiment, no adduct formation was observed at the same concentrations when PTDH was omitted from the solution.

Determination of Dissociation Constants for NAD^+, NADH, and Sulfite. Fluorescence titration experiments were performed to determine the affinity of NAD^+ and NADH

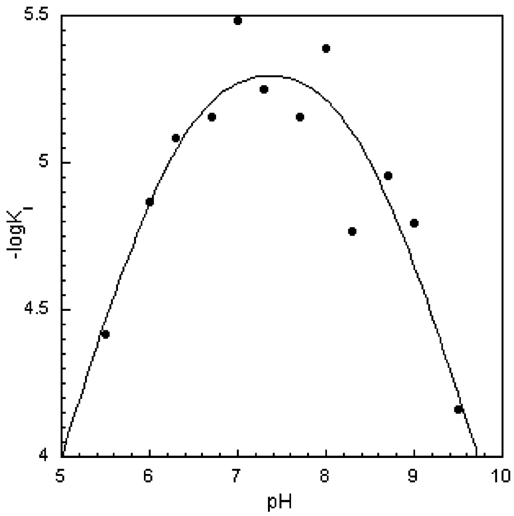

FIGURE 4: pH dependence of the inhibition constant of sulfite. The solid line was drawn by fitting the data to eq 2 (Experimental Procedures).

Table 2: Kinetic Isotope Effects at pH (pD) 7.25 and 8.0

parameter	pH	substrate KIE	SIE	substrate + solvent KIE	theoretical multiplicative result
k_{cat}	7.25	2.19 ± 0.06	1.55 ± 0.07	2.48 ± 0.11	3.39
$k_{cat}/K_{m,Pt}$	7.25	1.37 ± 0.28	4.38 ± 0.67	5.84 ± 0.93	
k_{cat}	8.0	1.80 ± 0.08	1.44 ± 0.07	1.76 (±0.09)	2.60
$k_{cat}/K_{m,Pt}$	8.0	1.43 ± 0.10	0.60 ± 0.04	0.53 (±0.04)	

for the free enzyme (Table 1). Both cofactors displayed micromolar dissociation constants, with NAD^+ binding somewhat more tightly. To decipher the binding order of substrates for PTDH as well as determine the apparent dissociation constant of the NAD^+−sulfite adduct, the apparent K_D values of NAD^+ in the presence and absence of sulfite were determined as well as the apparent dissociation constant of sulfite in the presence and absence of NAD^+. Sulfite by itself elicited only a very small change in fluorescence, which is attributed to a change in ionic strength. In the presence of saturating concentrations of NAD^+, addition of sulfite to the enzyme caused a much greater change in fluorescence (approximately 4-fold) and at much lower concentrations providing an apparent K_D of 0.6 μM. In the presence of sulfite, the binding affinity of NAD^+ was enhanced ∼20-fold (Table 1).

Substrate and Solvent Kinetic Isotope Effects. In a previous study, it was demonstrated using deuterium-labeled phosphite that the hydride from phosphite is directly transferred to the cofactor with *Re*-face stereospecificity (*3*). Kinetic isotope effects (KIEs) were observed on k_{cat} ($^{D}k_{cat} = 2.1 \pm 0.1$) and on $k_{cat}/K_{m,phosphite}$ ($^{D}k_{cat}/K_{m,phosphite} = 1.8 \pm 0.3$) at pH 7.25. No isotope effect was observed on $^{D}k_{cat}/K_{m,NAD^+}$. These findings were reproduced in this study, and KIEs were also determined at pH 8.0 [$^{D}k_{cat} = 1.80 \pm 0.08$ and $^{D}k_{cat}/K_{m,Pt} = 1.43 \pm 0.10$ (Table 2)].

Solvent kinetic isotope effects (SIEs) were measured by running identical reactions in buffers prepared with H_2O and D_2O. At pH (pD) 7.25, the enzymatic reaction exhibited normal isotope effects of 1.55 for k_{cat} and 4.38 for $k_{cat}/K_{m,phosphite}$ (Table 2). Deuterium oxide is a more viscous solvent than water, but a control reaction with 6% glycerol in water as a viscogen, resulting in a solution with the same measured viscosity as D_2O, indicated that the decrease in the kinetic parameters of the reaction in D_2O is caused by chemical and not physical factors. A reversal in the SIE was seen at pH (pD) 8.0, where $^{D_2O}(k_{cat}/K_{m,\ phosphite})$ was 0.60 and $^{D_2O}k_{cat}$ was 1.44 (Table 2).

Combined Substrate and Solvent Isotope Effects. In a concerted mechanism of phosphite oxidation, deprotonation of the water nucleophile and cleavage of the phosphorus hydrogen bond could occur in the same reaction step. To probe for this possibility, the kinetic parameters using deuterium-labeled substrate in D_2O were determined, providing values of 2.48 for $^{D,D_2O}k_{cat}$ and 5.84 for $^{D,D_2O}k_{cat}/K_{m,Pt}$ at pH 7.25. At pH 8.0, these values were 1.76 for $^{D,D_2O}k_{cat}$ and 0.53 for $^{D,D_2O}k_{cat}/K_{m,Pt}$ (Table 2).

DISCUSSION

Despite much effort, to date no alternative substrates have been uncovered for PTDH. In combination with the genetic context of the *ptxD* gene (*1*) and the observed upregulation of its expression in response to phosphate starvation (*36*), the physiological role of phosphite oxidation appears to be on solid ground despite a relatively low value for k_{cat}/K_m of 10^4 M^{-1} s^{-1}. This value is mostly depressed because of a relatively small k_{cat} (∼3−4 s^{-1}), especially in light of the strong driving force for the reaction. The observation of a KIE on k_{cat} does rule out the possibility that a slow physical step limits the rate of catalysis. The lack of alternative substrates presents a drawback with respect to mechanistic investigations as it has not proven to be possible to vary either the nucleophile or the hydride source.

Sulfite is a competitive inhibitor with respect to phosphite and an uncompetitive inhibitor with respect to NAD^+ (*2*). It has a trigonal pyramidal shape with a lone pair on sulfur and resembles phosphite, which carries a proton on that lone pair. Consistent with its uncompetitive inhibitory behavior with respect to NAD^+, the fluorescence titration experiments reported here essentially did not detect any significant binding of the compound to free enzyme, whereas strong binding was observed in the presence of NAD^+. These findings are consistent with the ordered bi-bi kinetic mechanism with NAD^+ binding first that was extracted from steady-state kinetic data (*2*). The binding of sulfite in the presence of NAD^+ is unusually tight (2 orders of magnitude below K_m for phosphite), and it also strongly enhances the binding of NAD^+ to well below its K_m value (Table 1). These findings suggested a possibly more complex inhibition scheme. Indeed, the increase in absorbance at 310 nm observed when a sample containing PTDH and NAD^+ was titrated with sulfite is consistent with the formation of a covalent adduct between sulfite and NAD^+ in which the sulfur atom is bound to C4 of nicotinamide (*37*, *38*). In the absence of the enzyme, the adduct was not observed under identical conditions, suggesting that PTDH catalyzes its formation, which is also supported by the lack of adduct formation with mutants His292Phe, His292Asn, and Arg237Lys. Adduct formation has also been reported for D-β-hydroxybutyrate DH (DHBDH) (*17*), malate DH, and L-lactate DH (*39*). The apparent binding constant for the adduct with PTDH is tighter (0.8 μM) than that with DHBDH (4 μM) and LDH (2 μM), which probably reflects the geometry of the active site of PTDH that evolved to accommodate three oxygens in a tetrahedral arrangement rather than two oxygens in a planar arrangement (carboxylate). The covalent adduct binds very tightly, as would be expected for a covalently linked two-substrate analogue (*40*, *41*). The adduct has been shown to be much less stable in solution ($K_a = 15$ mM) compared to the enzymes (*39*). Indeed, buildup of the free NAD^+–sulfite complex was not observed over time, explaining why sulfite inhibition is clearly uncompetitive with respect to NAD^+.

The pH–rate profile in Figure 3A shows that k_{cat} is independent of pH, indicating that the ternary complex composed of PTDH, NAD^+, and phosphite does not contain a solvent accessible group whose protonation state is critical for catalysis. The independence of k_{cat} on pH appears to contradict a previous study that reported a bell-shaped curve for the pH dependence of the specific activity of PTDH (*2*). All measurements in that study were taken at 1 mM phosphite and 0.5 mM NAD^+. Although these concentrations are saturating at the pH optimum, they are subsaturating at low and high pH values, resulting in an apparent reduction of activity, but this can be fully compensated by supplying high concentrations of both substrates.

In contrast to k_{cat}, $k_{cat}/K_{m,phosphite}$ is dependent on pH. The two proton transfer transitions observed in the bell-shaped curve in Figure 3B may correspond to deprotonation of either the substrate or the PTDH–NAD^+ complex with a pK_a of 6.8 and protonation of an enzyme residue with a pK_a of 7.8. The reported second acid dissociation constant of phosphorous acid is 6.8, and hence, the transition in the acidic limb of the pH–rate profile is consistent with the dianionic form of phosphite being the substrate of PTDH. The close correspondence between the pK_a of the free substrate and that observed in the $k_{cat}/K_{m,phosphite}$ profile also suggests that phosphite has a weak commitment to catalysis (is not a "sticky" substrate) since otherwise the latter pK_a would have been displaced outward (*15*). The substrate KIE observed on $k_{cat}/K_{m,phosphite}$ further corroborates the weak commitment to catalysis. The pH studies also clearly show that incorrectly protonated complexes of PTDH and phosphite do not form.

Unambiguous differentiation between a proton transfer event observed in k_{cat}/K_m occurring on the substrate or PTDH can be achieved by recording the pH dependence of the inhibition constant of a competitive inhibitor with respect to the substrate (*15*, *16*). If the observed pH dependence corresponds with the pK_a of the inhibitor, the transition observed in the pH–rate profile is shown to be associated with the substrate. On the other hand, if the pK_a observed with the inhibitor is identical to that observed for k_{cat}/K_m, then the proton transfer event is associated with a residue on the enzyme. When using this methodology, ideally one employs an inhibitor with an acid dissociation constant significantly different from that of the substrate such that the two scenarios can be readily distinguished. Unfortunately, the pK_{a2} of sulfurous acid, the only inhibitor uncovered thus far, is very close to that of phosphorous acid (6.8 vs 6.9) (*42*). The pK_a observed in the plot of K_i versus pH (Figure 4) is somewhat lower than this literature value.[2] Hence, although we think it is likely that the acidic limb of the k_{cat}/K_m–rate profile is associated with the substrate, we cannot unequivocally rule out the involvement of an enzyme residue.

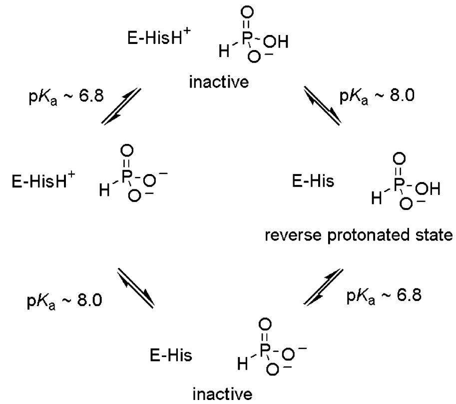

FIGURE 5: Possible protonation states of the phosphite substrate and PTDH. In a mechanism that utilizes a regular protonation state (left side), the dianionic form of phosphorous acid is the true substrate and an enzymatic residue must be protonated for binding. In a reverse protonation mechanism, the group with the lower pK_a, here phosphite mono anion, will remain protonated whereas the group with the higher pK_a, here a residue on PTDH, will be deprotonated in the active enzyme–substrate collision complex.

The basic limb of the curve for k_{cat}/K_m may represent a residue on the enzyme that must be protonated for phosphite binding to the PTDH–NAD^+ complex with a pK_a of around 8.0. Three potential candidates are the conserved residues His292, Arg237, and Lys76. Site-directed mutagenesis studies and the pH profiles displayed by the mutants of these residues rule out Lys76. However, these studies could not unambiguously assign this pK_a to His292 or Arg237 as mutants of His292 were inactive and the only active mutant of Arg237 was Arg237Lys, which exhibited a bell-shaped curve very similar to that of the wt enzyme (*9*). If this pK_a is due to Arg237, its value is significantly depressed from that in solution. There is, however, ample precedent that pK_a values of amino acid side chains can be strongly perturbed within enzyme active sites (*43*).

An interesting alternative explanation for the observed pH–rate profile on $k_{cat}/K_{m,phosphite}$ features a reverse protonated state as the active ternary complex (E·NAD^+·Pt). Whenever a pH–rate profile is bell-shaped with a separation of less than 2 pH units between the two pK_a's, one cannot readily distinguish between a normal protonation state in the enzyme–substrate complex and a reverse protonated state (Figure 5) (*16*). If the reverse protonated model were applied to PTDH, the monoprotonated form of phosphite would be the true substrate and a residue on the enzyme would be unprotonated for phosphite binding (Figure 5, right side) (*9*). In this mechanism, which provides explanations for the observed pH–rate profile with mutants, only a small fraction of the substrate and enzyme would be present in its correct protonation state at the pH optimum of 7.25, explaining why the catalytic efficiency of the enzyme is comparatively low despite the very strong thermodynamic driving force.

As with most enzymes that are believed to utilize a reverse protonation mechanism, one can wonder why PTDH would

[2] One possible explanation is that the measured K_i would not be a simple binding constant if the enzyme actually actively catalyzes the formation of the covalent adduct between NAD and sulfite. The fact that the adduct is not observed with mutants His292Phe, His292Asn, and Arg237Lys would be consistent with such an interpretation. The observed pH–K_i profile would then be a combination of binding and a follow-up chemical step, which may displace the observed pK_a.

operate by a reverse protonation mechanism. The answer may lie in the origin of the enzyme. Phosphite has yet to be reported as a constituent of the environment, but it has been used extensively in recent decades in industrial settings. Since phosphite is toxic to microorganisms such as the *Pseudomonas* strain from which PTDH was first isolated, it is conceivable that phosphite oxidation is a relatively recent activity that has not yet been fully optimized. Binding of phosphite in its monoprotonated form may therefore be a remnant of the monoanionic 2-keto acid substrate of its ancestor, although PTDH clearly has evolved to recruit an additional Lys to its active site. Furthermore, binding of the monoprotic form provides a clear avenue for converting an active site setup for oxidation of an alcohol substrate to one that would support oxidation of phosphite. An alternative explanation for the use of a reverse protonation mechanism is that the thermodynamic disadvantage of binding phosphite in its monoprotonated form may be offset by a kinetic advantage in catalysis. Unfortunately, unlike phosphoryl transfer reactions with heteroatom leaving groups (*44*, *45*), good model systems for providing insights into advantages that may be conferred onto the reaction by the protonation state of the substrate are not available. Clearly, verification that PTDH uses a reverse protonation mechanism by independently determining the pK_a of the active site residue, possibly using NMR methods, is essential. These studies are currently ongoing.

At both pH 7.25 and 8.0, PTDH exhibits small normal substrate KIEs on k_{cat} and $k_{cat}/K_{m,phosphite}$. As expected for an ordered mechanism with NAD^+ binding first (*46*, *47*), no isotope effect was observed on $k_{cat}/K_{m,NAD}$ when the second substrate phosphite was deuterated. Although small, the KIEs on k_{cat} and $k_{cat}/K_{m,phosphite}$ are considerable when taking into account the fact that P−H and P−D bonds are significantly weaker than C−H and C−D bonds. Taking the reported stretching frequencies of the P−H and P−D bonds observed by vibrational spectroscopy of phosphorous acid and its deuterium-labeled analogue (2457 and 1793 cm^{-1}, respectively) (*48*) as a measure of the difference in bond strengths, we determine the theoretical maximal KIE at 25 °C to be 5.1. The observation of normal isotope effects shows that despite the considerable driving force of the reaction, the chemistry of hydride transfer is at least partly rate limiting or it becomes rate limiting when deuterium-labeled phosphite is used. At both pH values, the KIE on k_{cat} is somewhat larger than that on $k_{cat}/K_{m,phosphite}$. This observation suggests that a step that is not part of k_{cat} masks the isotope effect in the latter case, which most likely is a conformational change prior to phosphite binding.

The overall reaction equation for the transformation catalyzed by PTDH (eq 1) clearly shows that a proton must be removed from water. To probe the kinetic importance of this deprotonation, PTDH was assayed in buffer prepared in D_2O. At pH 7.25, a large solvent isotope effect was observed for $k_{cat}/K_{m,phosphite}$ with a more modest value for k_{cat}. Given the shape of the pH dependence of $k_{cat}/K_{m,phosphite}$, the isotope effect on this parameter is a combination of both thermodynamic and kinetic factors (*49*), which complicates its interpretation. Because of the different acid dissociation constants for D_2O and H_2O, many functional groups have altered pK_a values in D_2O (usually approximately +0.4) (*22*). This affects both the enzyme and the substrate, whose pK_{a2} has been shown to increase by 0.55 unit when moving from H_2O to D_2O (*50*). In the context of the normal protonation mechanism in Figure 5, at pH 7.25 a greater proportion of phosphite is deprotonated in H_2O (pK_{a2} = 6.8) than in D_2O at pD 7.25 (pK_{a2} = 7.3). This thermodynamic effect decreases the dianionic substrate concentration in D_2O compared to H_2O and hence reduces the observed $k_{cat}/K_{m,phosphite}$ rate constant (normal isotope effect). This thermodynamic effect adds to any effect due to a kinetically important deprotonation event. Note that the same reasoning also applies to the reverse protonation model except that it would be an enzymatic residue that would be more deprotonated in H_2O than in D_2O.

The thermodynamic effect can sometimes be offset by performing the reaction in D_2O at a higher pD, but given the narrow bell-shaped curve of the pH dependence of $k_{cat}/K_{m,phosphite}$, attempts to this effect were unsuccessful as were attempts to deconvolute the thermodynamic and kinetic effects by performing a complete pH−rate profile experiment in D_2O. The effect of the pH dependence of $k_{cat}/K_{m,phosphite}$ on the observed SIE is illustrated well by the inverse value observed at pH 8.0 (0.60, Table 2). This inverse SIE can be mainly attributed to the change in pK_a of the group associated with the basic limb of the pH profile. At pH 8.0 in H_2O, this group is partially protonated (pK_a = 7.8), whereas at pD 8.0, the residue with an estimated pK_a in D_2O of 8.2 (7.8 + 0.4) is deprotonated to a much lesser extent, resulting in a faster rate in D_2O (inverse isotope effect).

Panels B and C of Figure 2 show two generic mechanisms for phosphite oxidation. These models are drawn for the normal protonation state, but corresponding mechanisms can readily be drawn for the reverse protonated mechanism and would not affect the following discussion. Regardless of whether the initial nucleophile is water or an enzymatic residue, several scenarios can be envisaged with regard to the details of the reaction mechanism (*51*). Nucleophile attack and hydride displacement can occur in concerted fashion or in a stepwise mode with a five-coordinate phosphorane intermediate (associative mechanism) or a metaphosphate intermediate (dissociative mechanism). A wealth of data argues against the intermediacy of metaphosphate in enzyme-catalyzed reactions, and hence, a stepwise dissociative reaction mechanism appears to be unlikely (*51*). In a concerted mechanism featuring water as the nucleophile, deprotonation and hydride transfer could occur in the same step (e.g., Figure 2B), whereas all other mechanisms would involve two separate steps for water deprotonation and hydride transfer (e.g., Figure 2C). Whenever two hydrogen transfer events occur in the same reaction step and this step is cleanly rate limiting, the combined isotope effect when both positions are labeled with deuterium will be the product of the kinetic isotope effects measured when either one of the positions is labeled (*52*, *53*). In the case of a concerted reaction of PTDH, the substrate KIE and solvent KIE would be multiplicative with the caveat that solvent isotope effects can involve effects other than the chemical proton transfer event. Hence, for completeness, we also determined the substrate KIE in D_2O. Given the complications in interpreting the SIE on $k_{cat}/K_{m,phosphite}$ discussed above, only the combined KIE on k_{cat} will be discussed. The kinetic SIE on k_{cat} is not complicated by thermodynamic effects because of the lack of a pH dependence on k_{cat}. At both pH and pD 7.25 and

8.0, the experimentally observed combined substrate and solvent KIEs are smaller than those predicted for a concerted process in which water deprotonation and hydride transfer occur in the same rate-limiting step. Hence, it is likely that the phosphite dehydrogenase reaction proceeds through a multistep kinetic mechanism.

SUMMARY

PTDH is highly specific for phosphite. Alternative substrates or nucleophiles have not been discovered so far, and none of the related members of the D-hydroxy acid dehydrogenases is capable of oxidizing phosphite. Sulfite is a potent inhibitor via formation of a covalent adduct with NAD^+ in the enzyme's active site. The pH−rate profile shows a pH-independent k_{cat} and a bell-shaped curve for $k_{cat}/K_{m,phosphite}$ with pK_a values of 6.8 and 7.8. Because of the close values of these pK_a's, two interpretations of these data are currently indistinguishable. In the most straightforward mechanism, the lower pK_a corresponds to deprotonation of the phosphite substrate whereas the higher pK_a is associated with an enzymatic residue. In a reverse protonated mechanism, a residue on the enzyme is responsible for the acidic limb, and deprotonation of monoanionic phosphite is associated with the basic limb. The latter model would explain the low values for $k_{cat}/K_{m,phosphite}$ despite a very strong thermodynamic driving force. The shape of the pH−rate profile of $k_{cat}/K_{m,phosphite}$ also results in large thermodynamic effects dominating the kinetic solvent isotope effects, which hampers its use in further defining the mechanism of the enzyme. The substrate kinetic isotope effects do show clearly, however, that chemistry is at least partially rate limiting despite the high exergonicity of the transformation, and they may allow further characterization of the kinetic mechanism via pre-steady-state investigations that are currently underway.

ACKNOWLEDGMENT

The fluorescence experiments were performed at the Laboratory for Fluorescence Dynamics (LFD) at the University of Illinois. The LFD is supported jointly by the National Center for Research Resources of the National Institutes of Health (Public Health Service Grant 5 P41-RRO3155) and the University of Illinois. We thank an anonymous referee for suggesting the reverse protonation model.

SUPPORTING INFORMATION AVAILABLE

pH dependence of $k_{cat}/K_{m,NAD}$. This material is available free of charge via the Internet at http://pubs.acs.org.

REFERENCES

1. Metcalf, W. W., and Wolfe, R. S. (1998) Molecular genetic analysis of phosphite and hypophosphite oxidation by *Pseudomonas stutzeri* WM88, *J. Bacteriol. 180*, 5547−5558.
2. Costas, A. M., White, A. K., and Metcalf, W. W. (2001) Purification and characterization of a novel phosphorus-oxidizing enzyme from *Pseudomonas stutzeri* WM88, *J. Biol. Chem. 276*, 17429−17436.
3. Vrtis, J. M., White, A., Metcalf, W. W., and van der Donk, W. A. (2001) Phosphite Dehydrogenase: An unusual Phosphoryl Transfer Reaction, *J. Am. Chem. Soc. 123*, 2672−2673.
4. Taguchi, H., and Ohta, T. (1991) D-Lactate dehydrogenase is a member of the D-isomer-specific 2-hydroxyacid dehydrogenase family. Cloning, sequencing, and expression in *Escherichia coli* of the D-lactate dehydrogenase gene of *Lactobacillus plantarum*, *J. Biol. Chem. 266*, 12588−12594.
5. Taguchi, H., and Ohta, T. (1993) Histidine 296 is essential for the catalysis in *Lactobacillus plantarum* D-lactate dehydrogenase, *J. Biol. Chem. 268*, 18030−18034.
6. Kochhar, S., Chuard, N., and Hottinger, H. (1992) Glutamate 264 modulates the pH dependence of the NAD^+-dependent D-lactate dehydrogenase, *J. Biol. Chem. 267*, 20298−20301.
7. Goldberg, J. D., Yoshida, T., and Brick, P. (1994) Crystal structure of a NAD-dependent D-glycerate dehydrogenase at 2.4 Å resolution, *J. Mol. Biol. 236*, 1123−1140.
8. Kochhar, S., Lamzin, V. S., Razeto, A., Delley, M., Hottinger, H., and Germond, J. E. (2000) Roles of His205, His296, His303 and Asp259 in catalysis by NAD^+-specific D-lactate dehydrogenase, *Eur. J. Biochem. 267*, 1633−1639.
9. Woodyer, R., Wheatley, J., Relyea, H., Rimkus, S., and van der Donk, W. A. (2005) Site-Directed Mutagenesis of Active Site Residues of Phosphite Dehydrogenase, *Biochemistry 44*, 4765−4774.
10. Woodyer, R., van der Donk, W. A., and Zhao, H. (2003) Relaxing the Nicotinamide Cofactor Specificity of Phosphite Dehydrogenase by Rational Design, *Biochemistry 42*, 11604−11614.
11. Kochhar, S., Hunziker, P. E., Leong-Morgenthaler, P., and Hottinger, H. (1992) Primary structure, physicochemical properties, and chemical modification of NAD^+-dependent D-lactate dehydrogenase. Evidence for the presence of Arg-235, His-303, Tyr-101, and Trp-19 at or near the active site, *J. Biol. Chem. 267*, 8499−8513.
12. Schütte, H., Flossdorf, J., Sahm, H., and Kula, M. R. (1976) Purification and properties of formaldehyde dehydrogenase and formate dehydrogenase from *Candida boidinii*, *Eur. J. Biochem. 62*, 151−160.
13. Walsh, D. A., and Sallach, H. J. (1965) Purification and properties of chicken liver D-3-phosphoglycerate dehydrogenase, *Biochemistry 4*, 1076−1085.
14. Ellis, K. J., and Morrison, J. F. (1982) Buffers of constant ionic strength for studying pH-dependent processes, *Methods Enzymol. 87*, 405−426.
15. Cleland, W. W. (1982) The use of pH studies to determine chemical mechanisms of enzyme-catalyzed reactions, *Methods Enzymol. 87*, 390−405.
16. Cleland, W. W. (1977) Determining the chemical mechanisms of enzyme-catalyzed reactions by kinetic studies, *Adv. Enzymol. 45*, 273−387.
17. Fritzsche, T. M., McIntyre, J. O., Fleischer, S., and Trommer, W. E. (1984) Complex formation between nucleotides and D-β-hydroxybutyrate dehydrogenase studied by fluorescence and EPR spectroscopy, *Biochim. Biophys. Acta 791*, 173−185.
18. Glasoe, P. K., and Long, F. A. (1960) Use of Glass Electrodes to Measure Acidities in Deuterium Oxide, *J. Phys. Chem. 64*, 188−191.
19. Dawson, R., Elliott, D., Elliott, W., and Jones, K. (1986) *Data for Biochemical Research*, 3rd ed., Oxford University Press, Oxford, U.K.
20. Robertson, J. G. (1979) *KinetAsyst*, Intellikinetics, State College, PA.
21. Cleland, W. W. (1979) Statistical Analysis of Enzyme Kinetic Data, *Methods Enzymol. 63*, 103−138.
22. Quinn, D. M., and Sutton, L. D. (1991) in *Enzyme Mechanism from Isotope Effects* (Cook, P. R., Ed.) pp 73−126, CRC Press, Boca Raton, FL.
23. Lakowicz, J. R. (1999) *Principles of Fluorescence Spectroscopy*, Kluwer Academic/Plenum, New York.
24. Seto, H., and Kuzuyama, T. (1999) Bioactive Natural Products with Carbon−Phosphorus Bonds and Their Biosynthesis, *Nat. Prod. Rep. 16*, 589−596.
25. Willems, H. A. M., Veeneman, G. H., and Westerduin, P. (1992) Synthesis of Racemic Myoinositol 1,4,5-Trismethylphosphonate, Myoinositol 4,5-Bismethylphosphonate and Myoinositol 5-Methylphosphonate Via a Phosphinate Approach, *Tetrahedron Lett. 33*, 2075−2078.
26. Seeberger, P. H., Jorgensen, P. N., Bankaitis-Davis, D. M., Beaton, G., and Caruthers, M. H. (1996) 5′-Dithiophosphoryl deoxyoligonucleotides: Synthesis and biological studies, *J. Am. Chem. Soc. 118*, 9562−9566.

27. Gerrard, A. F., and Hamer, N. K. (1968) Evidence for a Planar Intermediate in Alkaline Solvolysis of Methyl *N*-Cyclohexylphosphoramidothioic Chloride, *J. Chem. Soc. B*, 539−543.
28. Cullis, P. M., and Iagrossi, A. (1986) Thiophosphoryl-Transfer Reactions: Stereochemical Course of Solvolysis of *p*-Nitrophenyl Thiophosphate in Protic solvent and the Possible Role of Thiometaphosphate, *J. Am. Chem. Soc. 108*, 7870−7871.
29. Cullis, P. M., Misra, R., and Wilkins, D. J. (1987) Free Monomeric Thiometaphosphate in Protic Solvents: Complete Racemisation at Phosphorus in the Ethanolysis of 4-Nitrophenyl Thiophosphate, *J. Chem. Soc., Chem. Commun.*, 1594−1596.
30. Burgess, J., Blundell, N., Cullis, P. M., Hubbard, C. D., and Misra, R. (1988) Evidence for Free Monomeric Thiametaphosphate Anion in Aqueous Solution, *J. Am. Chem. Soc. 110*, 7900−7901.
31. Yang, Y. S., and Frey, P. A. (1990) Solvent Effects on the Solvolysis of ADPβS, *Bioorg. Chem. 18*, 373−380.
32. Banner, M. R., and Rosalki, S. B. (1967) Glyoxylate as a substrate for lactate dehydrogenase, *Nature 213*, 726−727.
33. Warren, W. A. (1970) Catalysis of both oxidation and reduction of glyoxylate by pig heart lactate dehydrogenase isozyme 1, *J. Biol. Chem. 245*, 1675−1681.
34. Lluis, C., and Bozal, J. (1977) Kinetic formulations for the oxidation and the reduction of glyoxylate by lactate dehydrogenase, *Biochim. Biophys. Acta 480*, 333−342.
35. Duncan, R. J., and Tipton, K. F. (1969) The oxidation and reduction of glyoxylate by lactic dehydrogenase, *Eur. J. Biochem. 11*, 58−61.
36. White, A. K., and Metcalf, W. W. (2004) The htx and ptx operons of *Pseudomonas stutzeri* WM88 are new members of the pho regulon, *J. Bacteriol. 186*, 5876−5882.
37. Pfeiderer, G., Jeckel, D., and Wieland, T. (1956) Action of sulfite on diphosphopyridine nucleotide (DPN) hydrogenating enzymes, *Biochem. Z. 328*, 187−194.
38. Carelli, V., Liberatore, F., Scipione, L., Musio, R., and Sciacovelli, O. (2000) On the structure of intermediate adducts arising from dithionite reduction of pyridinium salts: A novel class of derivatives of the parent sulfinic acid, *Tetrahedron Lett. 41*, 1235−1240.
39. Parker, D. M., Lodola, A., and Holbrook, J. J. (1978) Use of the sulphite adduct of nicotinamide-adenine dinucleotide to study ionizations and the kinetics of lactate dehydrogenase and malate dehydrogenase, *Biochem. J. 173*, 959−967.
40. Jencks, W. P. (1981) On the Attribution and Additivity of Binding Energies, *Proc. Natl. Acad. Sci. U.S.A. 78*, 4046−4050.
41. Jencks, W. P. (1975) Binding Energy, Specificity, and Enzymic Catalysis: The Circe Effect, *Adv. Enzymol. 43*, 219−410.
42. Lide, D. R. (1991) in *CRC Handbook of Chemistry and Physics*, CRC Press, Boca Raton, FL.
43. Fersht, A. (1985) *Enzyme Structure and Mechanism*, Freeman & Co., New York.
44. Cleland, W. W. (1990) Secondary ^{18}O isotope effects as a tool for studying reactions of phosphate mono-, di-, and triesters, *FASEB J. 4*, 2899−2905.
45. Williams, N. H. (2004) Models for biological phosphoryl transfer, *Biochim. Biophys. Acta 1697*, 279−287.
46. Northrop, D. B. (1977) in *Isotope Effects on Enzyme-Catalyzed Reaction* (Cleland, W. W., O'Leary, M. H., and Northrop, D. B., Eds.) pp 122−152, University Park Press, Baltimore.
47. Duggleby, R. G., and Northrop, D. B. (1989) The Expression of Kinetic Isotope Effects during the Time Course of Enzyme Catalyzed Reactions, *Bioorg. Chem. 17*, 177−193.
48. Martin, R. B. (1959) The Rate of Exchange of the Phosphorus Bonded Hydrogen in Phosphorous Acid, *J. Am. Chem. Soc. 81*, 1574−1576.
49. Schowen, K. B., and Schowen, R. L. (1982) Solvent isotope effects on enzyme systems, *Methods Enzymol. 87*, 551−606.
50. Salomaa, P., Hakala, R., Vesala, S., and Aalto, T. (1969) Solvent deuterium isotope effects on acid−base reactions. III. Relative acidity constants of inorganic oxyacids in light and heavy water. Kinetic applications, *Acta Chem. Scand. 23*, 2116−2126.
51. Relyea, H., and van der Donk, W. A. (2005) Mechanism and Applications of Phosphite Dehydrogenase, *Bioorg. Chem.* (in press).
52. Hermes, J. D., Roeske, C. A., O'Leary, M. H., and Cleland, W. W. (1982) Use of multiple isotope effects to determine enzyme mechanisms and intrinsic isotope effects. Malic enzyme and glucose-6-phosphate dehydrogenase, *Biochemistry 21*, 5106−5114.
53. Belasco, J. G., Albery, W. J., and Knowles, J. R. (1983) Double isotope fractionation: Test for concertedness and for transition-state dominance, *J. Am. Chem. Soc. 105*, 2475−2477.
54. Taguchi, H., Ohta, T., and Matsuzawa, H. (1997) Involvement of Glu-264 and Arg-235 in the essential interaction between the catalytic imidazole and substrate for the D-lactate dehydrogenase catalysis, *J. Biochem. 122*, 802−809.
55. Taguchi, H., and Ohta, T. (1994) Essential role of arginine 235 in the substrate-binding of *Lactobacillus plantarum* D-lactate dehydrogenase, *J. Biochem. 115*, 930−936.
56. Yoshida, T., Yamaguchi, K., Hagishita, T., Mitsunaga, T., Miyata, A., Tanabe, T., Toh, H., Ohshiro, T., Shimao, M., and Izumi, Y. (1994) Cloning and expression of the gene for hydroxypyruvate reductase (D-glycerate dehydrogenase from an obligate methylotroph *Hyphomicrobium methylovorum* GM2), *Eur. J. Biochem. 223*, 727−732.
57. Tobey, K. L., and Grant, G. A. (1986) The nucleotide sequence of the serA gene of *Escherichia coli* and the amino acid sequence of the encoded protein, D-3-phosphoglycerate dehydrogenase, *J. Biol. Chem. 261*, 12179−12183.
58. Bernard, N., Ferain, T., Garmyn, D., Hols, P., and Delcour, J. (1991) Cloning of the D-lactate dehydrogenase gene from *Lactobacillus delbrueckii* subsp. *bulgaricus* by complementation in *Escherichia coli*, *FEBS Lett. 290*, 61−64.
59. Popov, V. O., Shumilin, I. A., Ustinnikova, T. B., Lamzin, V. S., and Egorov, Ts. A. (1990) NAD-dependent formate dehydrogenase from methylotrophic bacteria *Pseudomonas* sp. 101. I. Amino acid sequence, *Bioorg. Khim. 16*, 324−335.

BI047640P